Early stages of glacial clustering in supercooled triphenyl phosphite

Birgit Effey Schwickert,[1] Steven R. Kline,[2] H. Zimmermann,[3] K. M. Lantzky,[4] and J. L. Yarger[4]
[1]*University of California at Berkeley, Department of Chemistry and Chemical Engineering, Berkeley, California 94720*
[2]*NIST Center for Neutron Research, Gaithersburg, Maryland 20899*
[3]*Max-Planck-Institut für Medizinische Forschung, 69120 Heidelberg, Germany*
[4]*University of Wyoming, Department of Chemistry, Laramie, Wyoming 82071*
(Received 25 October 2000; revised manuscript received 24 January 2001; published 2 July 2001)

Glacial phase clustering and growth in triphenyl phosphite is observed in the temperature interval of 210 K to 214 K by small angle neutron scattering performed at the NIST Center for Neutron Research. Presented are the radius, volume fraction, and polydispersity of clusters of glacial phase surrounded by a supercooled liquid. The data can be interpreted in a four-step model of (I) cluster formation, (II) rapid nucleation, (III) agglomeration, and finally (IV) saturation. Two schemes of cluster growth can be identified. The first one is a region of radius stagnation (II), which is followed by a region of volume stagnation (III). Competition between the increase in cluster size and the increase in the number of clusters is deduced from this behavior.

DOI: 10.1103/PhysRevB.64.045410 PACS number(s): 61.46.+w, 71.55.Jv, 61.20.Lc, 61.12.Ex

I. INTRODUCTION

Clusters have become increasingly popular subjects for investigation, partly because of their novel status of being intermediate between molecular and bulk systems and partly because of their interesting growth properties. Notably, in the research areas of supercooled liquids attention has been focused on models[1,2] to describe the process of cluster formation but only a few experiments[3] have been performed to distinguish between different models. This work, a small angle neutron scattering (SANS) study of supercooled triphenyl phosphite [$P(OC_6H_5)_3$, abbreviated as TPP], gives insight into the early stages of cluster formation.

The existence in TPP of a glacial state that is distinct from the glass originally caused the proposal that TPP belongs to the class of polyamorphous materials,[4] i.e., the existence of two or more amorphous states in a glass-forming material. However, further investigation has shown that the glacial phase of TPP is not truly amorphous but rather is characterized by nanocrystallized domains.[5] Kivelson and co-workers[6] have speculated that this glacial state could be the experimental realization of a defect-ordered crystal as predicted by the frustration-limited domain theory[2] and characterized by an unusually large unit cell. Such a physical picture could also explain the giant Fischer clusters[7] observed in other supercooled liquids.[8] This second phase, commonly called a glacial phase, is distinct from and denser than both the ordinary supercooled liquid and the glass and displays many unusual properties.[9,10] During the glaciation process the sample first gets cloudy, then turns nearly opaque, and eventually clears up again. Evidence from light scattering exists for the presence of clusters of remarkable size, several hundred nanometers, in the early stages of the transition from the supercooled liquid to the glacial phase. Those clusters are believed to be ''pieces'' of the glacial phase.

Theory by Fischer and co-workers[2] on frustation-limited clusters was applied to TPP (Ref. 6) in which intensities of light scattering experiments are ascribed to frustrated superclusters, agglomerates of smaller primary clusters. Correlation lengths of 1000 nm after 3 h at 215 K were recorded. An interpretation of an x-ray study[11] of TPP suggested correlation lengths of 30 Å in the temperature regime of 210 K to 216 K. Oguni and co-workers[1,12] introduced a model for intracluster rearrangement for the α process in supercooled liquids and applied it to the glacial phase of TPP. Two processes are proposed to compete with each other: the rearrangement motion of a few molecules within a cluster and the process to change cluster size. The finite size of clusters is explained in many different ways, one of which is by frustration, the inability to extend the locally preferred structure through space.[2] Others[11] speculate on a competition between volume and area forces.

This work focuses on cluster growth in supercooled TPP in the temperature range of 210 K to 214 K. SANS data are shown and interpreted using modeling. Cluster growth can be envisioned in four stages: (I) cluster formation, (II) rapid nucleation, (III) agglomeration, and finally (IV) saturation. Most remarkable behaviors are found during the rapid nucleation and agglomeration periods and will be discussed in detail in the Results section.

II. EXPERIMENTAL METHODS AND SANS DATA REDUCTION

TPP and perdeuterated TPP samples were prepared by reacting either phenol or d_6-phenol (Aldrich Chemical) with phosphorous trichloride (Alfa Aesar) under an inert atmosphere at room temperature for 1 h. Vacuum distillation was used to purify the product. The purity of TPP samples was determined by ^{1}H and ^{31}P NMR to be 99+%. A TA Instruments 2920 differential scanning calorimetry was used to measure the glass transition temperature (T_g) of pure TPP. The glass transition temperature was determined to be 200 K$\pm$2 K using a scanning rate of 20 K/min. Furthermore, the glacial phase and melting point transitions were observed when following the DSC scanning schedule outlined by Kivelson and co-workers.[6]

TPP was filled into a 5 mm path length SANS cell in a

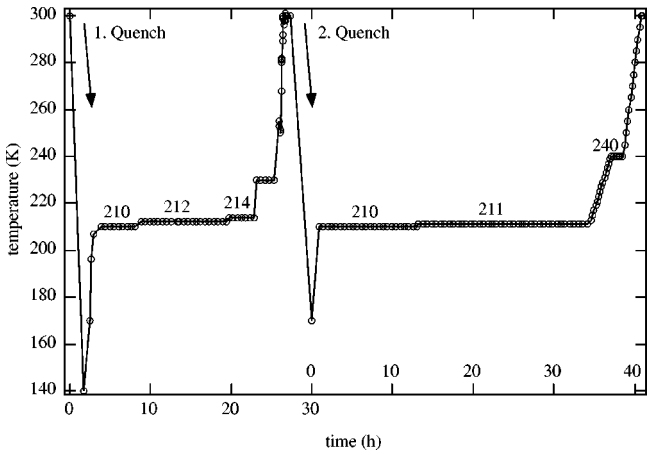

FIG. 1. The temperature profile of the two SANS runs are displayed versus time where time zero equals the coldest sample temperature in the glass state. Each circle represents one measurement.

glove box of approximately 5 ppm oxygen and moisture content. The cell was then placed into an aluminum sample container, which was sealed with an indium o-ring and leak checked. Special quench procedures were undertaken to accomodate a sufficient quench rate as well as keeping the sample container clean of moisture condensation. The sample temperature was monitored with a calibrated diode. A separate experiment showed that the temperature at the bottom of the sample can was within 0.1 K of the temperature where the thermometer was mounted during the actual experiment.

Small angle neutron scattering experiments were performed on the 8 m SANS spectrometer at the Center for Neutron Research at the National Institue of Standards and Technology (NIST). The detector is a 64×64 cm^2 position-sensitive proportionality counter with a spatial resolution of 10 mm. All measurements were taken with a wavelength of 5 Å with a wavelength resolution $\Delta\lambda/\lambda=0.25$. The wavelength spread, the collimation optics, and the detector resolution contribute to the overall instrumental smearing, but do not have a significant effect on the observed scattering from TPP. Half-hour SANS spectra were continuously accumulated.

Two SANS runs were performed with similar temperature profiles in the range of 210 K to 214 K, the low-temperature end of the glacial phase (see Fig. 1). After the first run, the sample was heated to 300 K. During this warming process, SANS intensities were monitored carefully to ensure that the sample was fully transformed to its original liquid state before the second run started.

A background spectrum of the glass state at 170 K was subtracted from the SANS data to correct for instrumental background and transmission effects. To obtain the one-dimensional scattering function, $I(Q)$, circular averages were calculated after reducing the data with a sensitivity and mask file. The intensities could not be converted to absolute values since no standard sample was measured and spectra shown in this work are therefore on an arbitrary intensity scale. It should be noted that uncertainties in the reduced data in the early stages of cluster formation are large owing to low scattering intensities. These large uncertainties only affect stage 1 of cluster formation.

III. SANS ANALYSIS

The measured differential scattering cross section per unit volume, $I(q)$, as a function of momentum transfer, q [$q=(4\pi/\lambda)\sin(\theta/2)$], where θ is the scattering angle and λ is the neutron wavelength, is proportional to the density of the particles, N, the intraparticle structure factor, $P(q)$, and the interparticle structure factor, $S(q)$:

$$I(q)=NP(q)S(q). \tag{1}$$

For dilute systems, where the interparticle interaction is negligible, $S(q)$ approaches unity and the intraparticle structure factor is the only one influencing the scattering cross section. In this case, the Guinier approximation for small q ranges ($q_{\max}R_g<1$) can be applied. Information on the radius of gyration of the scattering particles, R_g, can be determined from the slope of $\ln[I(q)]$ vs q^2 according to

$$I(q)=I(0)e^{-q^2R_g^2/3}, \tag{2}$$

where $I(0)=NV^2(\Delta\rho)^2$ is the coherent scattering at zero angle, N is the number of particles per unit volume, V is the volume of the particle, and $\Delta\rho$ is the difference in the scattering length densities of the particle and the solvent. For spherical particles, $R_g=\sqrt{3/5}R$ with R being the radius of the sphere. In the case of TPP, the Guinier approximation was applicable only for the first few measurements at 210 K to 212 K. Thereafter, scattering intensities were found to drop significantly in the low-q range pointing to the fact of strong volume interactions (see Fig. 2).

Scattering data were fitted using two models: the first of polydisperse hard spheres using the Percus-Yevick closure[13] and the second of monodisperse fractal clusters.[14] At the early stages of growth, each model fitted the data equally well, yielding nearly identical radii. The fitted fractal dimension was not statistically different from four, consistent with scattering from a nonfractal object. Further, the fractal model was incapable of modeling the emerging peak in the scattering spectra at later stages of growth. For these reasons all of the data are modeled using the polydisperse hard sphere model, detailed below, providing a continuous description of all stages of cluster growth.

The scattering intensity from a system containing a continuous distribution of particles with diameters σ_i and scattering amplitude $F_i(q)$ is given by

$$I(q)=N\int_0^\infty F_i^2(q)f(\sigma_i)d\sigma_i + N\int_0^\infty\int_0^\infty F_i(q)F_j(q)H_{ij}(q)f(\sigma_i)f(\sigma_j)d\sigma_i d\sigma_j, \tag{3}$$

where $\vec{q}$ is the wave vector, $H_{ij}(q)$ is the pair structure tensor, and $f(\sigma_i)$ and $f(\sigma_j)$ are the distribution functions of particles i and j, respectively. The volume fraction, ϕ, is

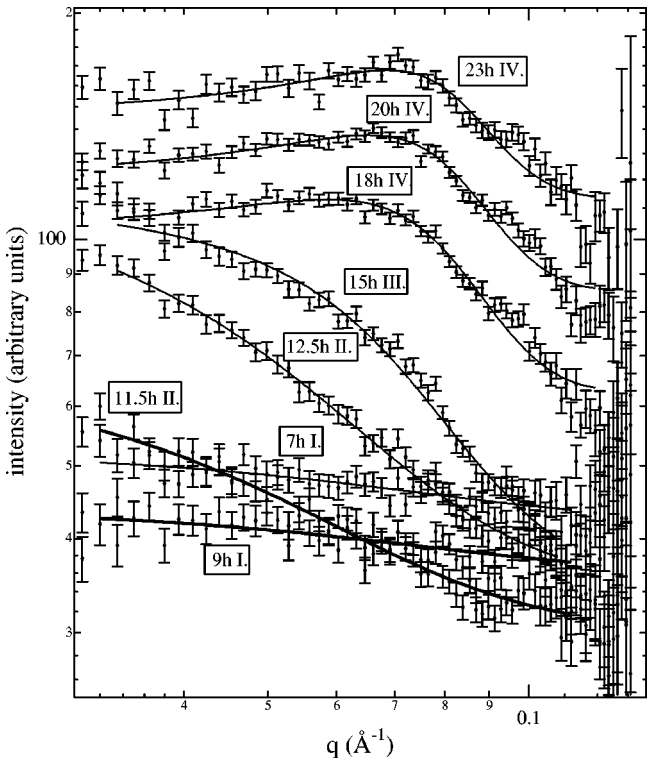

FIG. 2. Examples of SANS data taken at different times and their fits are shown for TPP at 210 K to 214 K. The data fits were created using the polydisperse hard sphere model using the following fixed parameters: (contrast)×(scale factor)=7×10^{-6} Å^{-2} and polydispersity = 0.6 (7 h, 9 h, 11.5 h, 12.5 h), 0.3 (15 h), 0.05 (18 h, 20 h, and 23 h).

equal to NV_{avg}. This model includes hard sphere interactions between particles and uses a Schulz distribution to describe the polydispersity of the radius. For a Schulz distribution, the probability density function is given by

$$f(\sigma)=\frac{\sigma^{c-1}e^{-\sigma/b}}{b^{c}\Gamma(c)}, \tag{4}$$

where b and c are given by $b=\sigma_{\text{mean}}/(z+1)$ and $c=z+1$, with z being the Schulz width factor. The intensity of neutron scattering is directly proportional to the square of the contrast, i.e., the square of the difference in scattering length densities between the particles and the solvent (in the case of TPP, between clusters of glacial phase and surrounding supercooled liquid):

$$\text{contrast}=(\rho_1-\rho_2)\quad\text{with}\quad\rho_i=\sum_{i=1}^{n}b_i\frac{\rho_b N_A}{M}, \tag{5}$$

with b_i is the scattering length of atom i, n the total number of atoms in the molecule, ρ_b the bulk density, and M the molar mass. For this work an intensity calibration run was not performed; the acquired intensities are arbitrary and therefore a contrast cannot be extracted. Nevertheless, a contrast for TPP was estimated to ensure that the features seen with SANS are physically plausible. No experimental data on densities in the glacial phase and supercooled liquid at 210 K were found in the literature. The densities used here are based on information given by Ref. 10 on density measurements of the supercooled liquid down to 245 K and Ref. 11 on observed shifts in x-ray scattering peaks of the crystal and glacial phase. Estimates at 210 K were calculated to 1.258 g/cm^3 (supercooled liquid), 1.306 g/cm^3 (crystal), and 1.281 g/cm^3 (glacial phase). It should be noted that these density estimates disagree with the speculation by Kivelson and co-workers that the glacial phase is denser than the crystal (Ref. 6, p. 8525). The scattering length density of the supercooled liquid is 5.64×10^{-6} Å^{-2} and of the glacial phase is 5.75×10^{-6} Å^{-2}. A contrast between the supercooled liquid and the glacial phase can be calculated to 1.1×10^{-7} Å^{-2}. For modeling the TPP SANS data, all of the data sets were fitted using a single value ($=7\times10^{-6}$ Å^{-2}) for the product of the (unknown) scaling factor times the calculated contrast, implying that the densities of the supercooled liquid and the glacial phase were constant over a 24 hour time period. Of the five fitting parameters of the polydisperse hard sphere model, the radius, volume fraction, background, polydispersity, and contrast, the last two were held fixed. Each data set was fitted with a variety of polydispersities (during each of those fits, the polydispersity was held fixed) from which the one with the best χ^2 was selected. Holding contrast and polydispersity fixed, the polydisperse hard sphere model extracts radius, volume fraction, and background from the fit. Examples of fits to the data are displayed in Fig. 2. The peak around 0.1 Å^{-1} appears to be an artifact of the detector, and is not considered in the analysis.

IV. RESULTS AND DISCUSSION

Figure 3 represents a summary of volume fraction, radius, polydispersity, and temperature data obtained from the polydisperse hard sphere fit. Raw data curves of the two runs highlighting the different cluster growth stages are displayed in Fig. 4. Accordingly, glacial cluster growth and agglomeration can be categorized into four steps: (I) cluster formation, (II) rapid nucleation, (III) agglomeration, and (IV) saturation. The interpretation of these individual processes can be visualized by the schematic in Fig. 5 and will be discussed in detail in the following.

A. Cluster formation

Only a few small and very polydisperse clusters are observed during the first 6 hours at 210 K and 211 K (see region I of Fig. 3). At the beginning only 3% of the sample contributes towards signal giving rise to large uncertainties. The relative magnitude of this number should not be underestimated though. For 1/2 g of deuterated TPP, 3% is equivalent to 2.8×10^{19} molecules participating in cluster formation. Further information can be obtained by comparing the two runs. The time scale of the second run had to be shifted backwards by 10 hours, i.e., the increase in cluster size and volume fraction and decrease in polydispersity during the second run occurred 10 hours later than in the first run. (Succeeding referrals to times are based on the unshifted

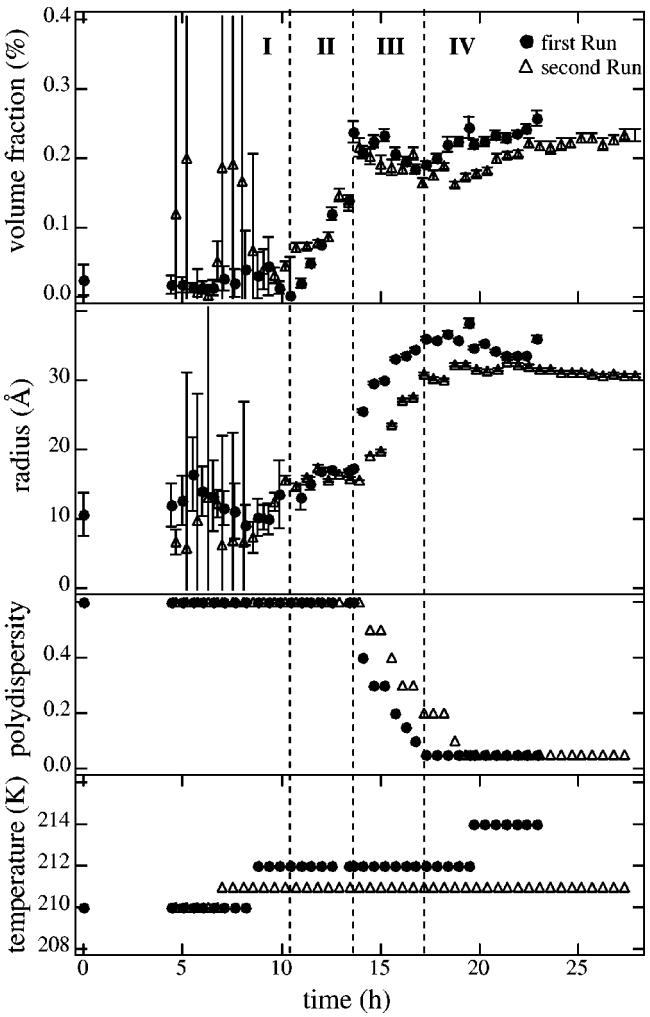

FIG. 3. Sample temperature, polydispersity, radius and volume fraction of glacial clusters are shown versus time.

first run. The complete, unshifted temperature data are shown in Fig. 1.) This seemingly arbitrary time shift is suspected to be due to uncontrollable influences on nucleation events. However, once nucleation is activated in both runs, the cluster growth is remarkably similar.

The mean radius of glacial clusters stays around 10 Å to 14 Å, retaining a high polydispersity. Polydispersity is on a 0 to 1 scale and can be converted to variations in radius as follows:[15] $\sigma = (\text{polydispersity}) \times R_{\text{mean}}$. For a mean radius of 10 Å (14 Å) a polydispersity of 0.6 translates into a variance of 6 Å (8.4 Å). Information on cluster growth behavior cannot be retrieved in this early stage owing to the large uncertainties induced by low volume fractions.

B. Rapid nucleation

A closer look at this intermediate stage reveals a radius plateau in both runs in the time window of 10 hours to 14 hours. Noteworthy is that the constant mean radius (16 Å) during this period is about half the radius of the final state of 30 Å. Even more striking is the growth in volume. A radius increase from 14 Å to 16 Å from stage (I) to (II) cannot account for a volume expansion of about 10%. Hence this must mean, keeping the high polydispersity of 9.6 Å in mind, that new clusters are forming while existing ones grow, keeping an average radius of 16 Å.

C. Agglomeration

In region III of Fig. 3, the volume fraction stays at its maximum, with an abrupt increase in radius and drop in polydispersity. During this time period clusters may rearrange, combine with close by clusters to double their size, and reach their equilibrium, final state, on a time scale of 28 hours, maintaining a constant volume. To further support the idea of agglomeration, the total number of clusters at a given time $N_c(t)$ can be calculated from the volume fraction and mean radius information of the SANS data. Assuming a spherical TPP molecule of 10 Å diameter, the problem of calculating the number of TPP molecules that fit into a sphere of 20 Å or 60 Å is not trivial. With the principle of a closest packed structure, the number of TPP molecules per cluster can be approximated to 5 and 153, respectively, and the number of clusters can be readily calculated. $N_c(t)$ is displayed in Fig. 6 and cannot be represented by any kind of simple function such as an exponential. It rather shows a maximum after 14 h, followed by a steep decrease (this is the agglomeration region) and a soft increase before reaching saturation. The ability of clusters to rearrange themselves in a fashion that allows the construction of just 60 Å clusters is quite a remarkable behavior. During this process the polydispersity drops from 9 Å at a mean radius of 15 Å to 1.5 Å at a mean radius of 30 Å.

D. Saturation

Clusters have large size distributions during the first 15 hours of their growth, however, after reaching 30 Å to 35 Å they stop growing and combine with a notably uniform diameter. Not only is the agglomeration process terminated but also no evidence for the emergence of smaller clusters is found since the volume fraction stays constant. The 30 Å clusters are spatially separated by supercooled liquid. The spatially separation of clusters can be deduced from the fact that the peak at around 0.07 Å^{-1} (see Fig. 2, 18 h, 20 h, and 23 h curves) does not shift. It should be pointed out that small temperature variations for the two runs in the range of 210 K to 214 K do not influence the growth rate, the size, or the volume fraction of the glacial phase.

The observed final cluster size of 60 Å of this work should be compared to the coherence length of 30 Å observed by Hedoux *et al.*[11] Taking a closer look at the x-ray data provided by this group,[11] the discrepancy might be on account of several x-ray specific features and data collection procedures. The time it takes to accumulate each x-ray pattern was 5.6 h to 11.1 h, averaging over several SANS data sets, each 0.5 h in length. It appears that the data were collected after a wait of up to 12 h, which would bring the collection period to the third phase in the SANS data and a mean radius of 16 Å, a diameter of 32 Å, and good agreement with x-ray data. No uncertainties were provided with

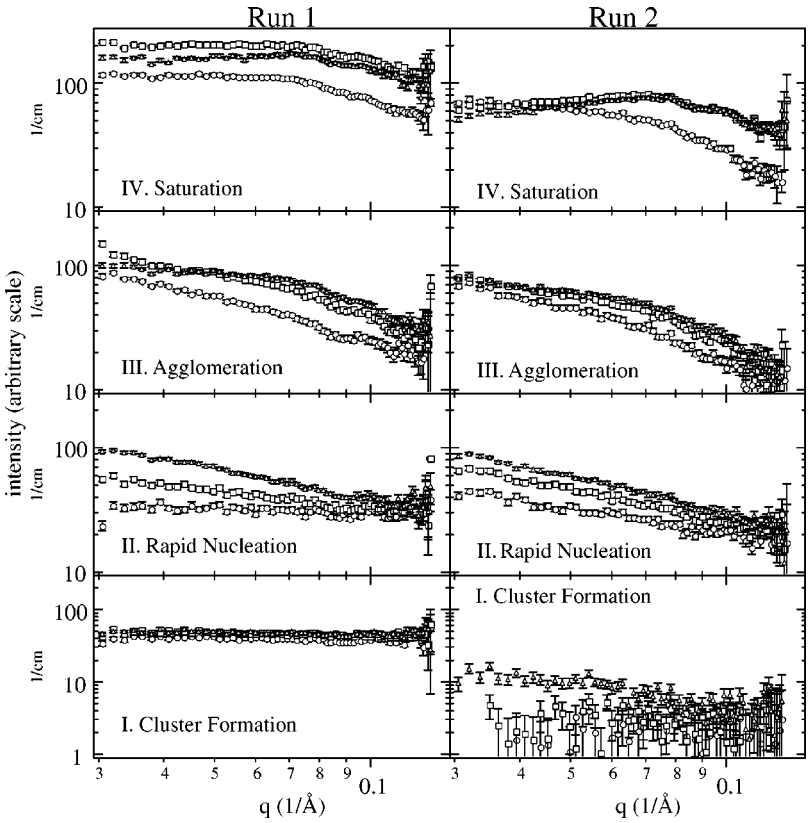

FIG. 4. Raw data curves of the two SANS runs are displayed. Each growth stage is illustrated in a separate graph with data from the beginning (circles), middle (squares), and end (triangles) of the phase.

the x-ray deduced approximate coherence lengths. A constant final cluster size in the temperature interval of 210 K to 216 K was observed.[11] Agreeably, the two SANS runs, having different temperature profiles in the range of 210 K to 214 K, do not show any dependency of cluster size on temperature. Next to cluster sizes, SANS was able to provide polydispersities of clusters and volume fractions. The suggestion by Kivelson and co-workers[6] and Fischer and co-workers[2] that the number and size of clusters increase with time can be partially confirmed. Glacial polydisperse clusters of 20 Å diameter reach uniform 60 Å clusters after 28 hours. However, the number of clusters decreases with increasing time as clusters agglomerate. This observation of rearrangement of near by smaller clusters to form larger ones on the length scales of Å could be envisioned on a larger light scattering length scale by studying cluster growth at higher temperatures as Kivelson and co-workers did. Therefore, the concept is in close relation to the theories by Kivelson and co-workers on superclusters in the hundreds of nanometers being composed of primary clusters. The question of why clusters in a temperature range of 210 K to 214 K stop growing at 60 Å still needs to be addressed. The present work can only contribute in that the possibility of cessation in cluster growth is not dependent on clusters col-

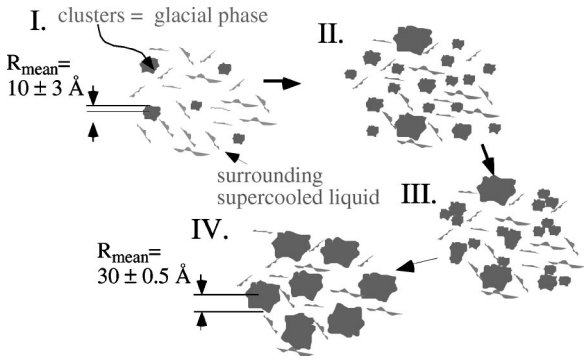

FIG. 5. A diagram of glacial cluster growth is shown at different stages. Clusters detected by SANS are pieces of the glacial phase surrounded by supercooled liquid. Different stages of cluster growths are pointed out.

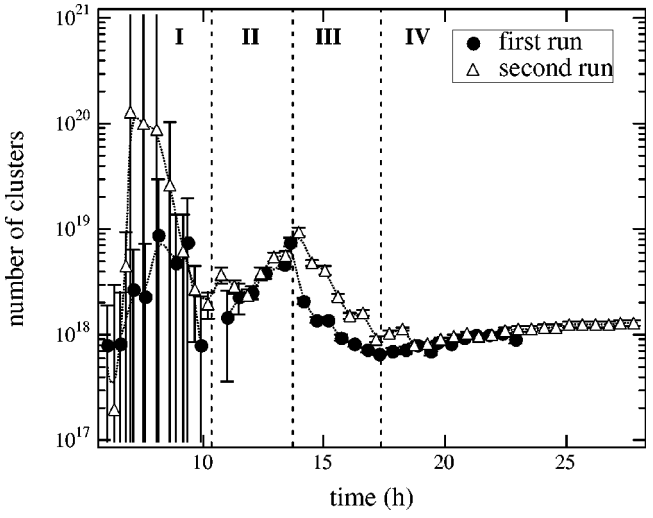

FIG. 6. The total number of clusters at any given point of time is illustrated. On account of large error bars, points below 6 h are not presented.

liding into each other, which can be ruled out by the spatial separation of 60 Å clusters. The speculation by Hedoux *et al.* of competition between volume and area forces seems plausible.

V. CONCLUSIONS

Glacial clustering in TPP in the temperature interval of 210 K to 214 K was observed by small angle neutron scattering. Applying a polydisperse hard sphere model to the data, the radius, volume fraction, and polydispersity were extracted and monitored over a 28 hour time period. The data were interpreted via a four-stage model, including cluster formation, rapid nucleation, agglomeration, and saturation. Nucleation starts arbitrarily for the two runs pointing to the fact that the onset of cluster growth is influenced by external parameters. Few clusters of diverse radii form in the supercooled liquid giving rise to a high polydispersity. Reaching the nucleation period, new clusters form while existing ones keep growing retaining a mean radius of 16 Å. Reaching a volume fraction of 25%, agglomeration of clusters occurs leading to very uniform 60 Å clusters, which is the end of any detectable activity in TPP.

ACKNOWLEDGMENTS

This work was supported by the Miller Institute for Basic Research in Science, the Dreyfus Foundation, the ACS Petroleum Research Fund (Grant No. 35819-G5), the National Science Foundation (Grant No. 0094202), and the Department of Energy (Grant No. ER 45836). We acknowledge the support of the National Institute of Standards and Technology, U.S. Department of Commerce, in providing the neutron research facility used in this work. The identification of any commercial product or trade name does not imply endorsement or recommendation by the National Institute of Standards and Technology. We would like to thank Professor Ron Cappelletti for his significant input to both experiment and discussion of this work. We also wish to thank Dr. Charlie Glinka, Dr. Dan Neumann, Dr. Mike Toney, and Professor Erich Roessler and his group for useful discussions. Thanks are due Louis Santodonato for calibrating the thermocouple. B.E.S. would like to thank Professor Jeff Reimer and Professor Alex Pines for providing resources and intellectual input on this project.

[1] Masaharu Oguni, J. Non-Cryst. Solids **210**, 171 (1997).

[2] Steven A. Kivelson, Xiaolin Zhao, Daniel Kivelson, Thomas M. Fischer, and Charles M. Knobler, J. Chem. Phys. **101**, 2391 (1994).

[3] For example: Bernd Schiener, Alois Loidl, Ralph V. Chamberlin, and Roland Boehmer, J. Mol. Liq. **69**, 243 (1996).

[4] J. L. Yarger, C. A. Angell, S. S. Borick and G. H. Wolf, in *Supercooled Liquids: Advances and Novel Applications*, edited by J. T. Forukas, D. Kivelson, U. Mohanty, and K. A. Nelson, (ACS Publications, Washington, D.C. 1997), Vol. 676, Chap. 16; C.A. Angell, Physica D **107**, 122 (1997); Y. Katayama, T. Mizutani, W. Utsumi, O. Shimomura, M. Yamakata, and K. Funakoshi, Nature (London) **403**, 170 (2000); H. Tanaka, Europhys. Lett. **50**, 340 (2000).

[5] A. Hedoux, O. Hernandex, J. Lefebvre, Y. Guinet, and M. Descamps, Phys. Rev. B **60**, 9390 (1999).

[6] A. Ha, I. Cohen, X. Zhao, M. Lee, and D. Kivelson, J. Phys. Chem. **100**, 1 (1996); Itai Cohen, Alice Ha, Xiaolin Zhao, Michelle Lee, Thomas Fischer, M. Jane Strouse, and Daniel Kivelson, *ibid.* **100**, 8518 (1996).

[7] D. Kivelson, J. Pereda, K. Luu, M. Lee, H. Sakai, A. Ha, I. Cohen, and G. Tarjus, in *Supercooled Liquids: Advances and Novel Applications*, edited by J. T. Forukas, D. Kivelson, U. Mohanty, and K. A. Nelson (ACS Publications, Washington, D.C. 1997), Vol. 676, Chap. 16.

[8] P. Poole, U. Essmann, F. Sciortino, and H. Stanley, Phys. Rev. E **48**, 4605 (1993).

[9] For example: J. Wiedersich, A. Kudlik, J. Gottwald, G. Benini, I. Roggatz, and E. Roessler, J. Phys. Chem. B **101**, 5800 (1997); S. Dvinskikh, G. Benini, J. Senker, M. Vogel, J. Wiedersich, A. Kudlik, and E. Roessler, *ibid.* **103**, 1727 (1999); Itai Cohen, Alice Ha, Xiaolin Zhao, Michelle Lee, Thomas Fischer, M. Jane Strouse, and Daniel Kivelson, J. Phys. Chem. **100**, 8518 (1996); A. Hedoux, Y. Guinet, and M. Descamps, Phys. Rev. B **58**, 31 (1998); G.P. Johari and C.J. Ferrari, J. Phys. Chem. B **101**, 10 191 (1997); Mayumi Mizukami, Kazuhisa Kobashi, Minoru Hanaya, and Masaharu Oguni, *ibid.* **103**, 4078 (1999).

[10] Philip J. Chappell, Michael P. Allen, Robert I. Hallem, and Daniel Kivelson, J. Chem. Phys. **74**, 5929 (1981).

[11] A. Hedoux, Y. Guinet, and M. Descamps, Phys. Rev. B **58**, 31 (1998).

[12] Mayumi Mizukami, Kazuhisa Kobashi, Minoru Hanaya, and Masaharu Oguni, J. Phys. Chem. B **103**, 4078 (1999).

[13] W. L. Griffith, R. Triolo, and A. L. Compere, Phys. Rev. A **35**, 2200 (1987).

[14] J. Teixeira, J. Appl. Crystallogr. **21**, 781 (1988).

[15] J. Hayter, in *Physics of Amphiphiles—Micelles, Vesicles and Microemulsions*, edited by V. DeGiorgio and M. Corti (Elsevier Science Publishers, Amsterdam, The Netherlands, 1985), 1983), p. 69.